COMPARISON OF CRACK-TIP STRESS EVALUATION METHODS IN ELASTIC-PLASTIC AND CREEP CONDITIONS ON CT SPECIMENS

L. LAIARINANDRASANA*, R. PIQUES**, B.DRUBAY*

In the nuclear industry, the behaviour of crack like defects in components operating at high temperature must be under control. Some methods for calculating the time of crack initiation from pre-existing defects are needed. For this purpose, correlation is checked between Ti (initiation time) and local parameters such as the largest principal stress at a characteristic finite distance d from the crack-tip (σ_d criterion) [1].
This paper compares two methods for calculating this largest principal stress (for $\theta = 0$ see **fig.1** for θ definition) : finite element analysis and theoretical methods (stress fields described by Hutchinson et al(HRR) [2] or by Riedel and Rice (RR) [3]).
Results were used for analysing correlation between Ti and the largest principal stress, in order to compare it with the nominal stress versus time to failure curve for smooth specimens.

1.INTRODUCTION

The behaviour of crack like defects in components operating at high temperature where creep is significant must be under control. Some methods for calculating the time of crack initiation from pre-existing defects are needed. For this purpose, an important test program named AMORFIS has been performed, at CEA Saclay, on 316L(N) austenitic stainless steel CT specimens operating at high temperature under monotonic and cyclic loadings with or without holdtime. In this paper, we are interested in pure creep tests at 650°C. Based on these tests, correlation is checked between Ti (initiation time) and local parameters such as the largest principal stress at a characteristic finite distance d from the crack-tip (σ_d criterion) [1].

Two methods were used in order to calculate the largest principal stress : finite element analysis and theoretical methods (stress fields described by Hutchinson et al (HRR) [2] or by Riedel and Rice (RR) [3]). In fact, calculations have to be performed with two steps : the initial loading (plasticity) and the actual creep test.

* CEA/DMT - CEN SACLAY 91191 GIF sur YVETTE cedex FRANCE
** Centre des Matériaux EMP, URA CNRS n°866 91003 Evry Cedex, FRANCE

2. EXPERIMENTAL PROCEDURES

2.1.Material

The alloy which is an 316L(N) type stainless steel was provided in a 30mm thick rolled plate in an annealed conditions (annealed at 1100°C and water-quenched).

TABLE 1 - 316L(N) chemical composition (Wt. Pct.)

C	Ni	Cr	Mn	Cu	Si	Ti	S	P	Mo	Co	Nb	Ta	N2	B
0.02	12.2	17.51	1.76	0.13	0.35	0.004	0.004	0.021	2.35	0.11	0.005	<0.01	0.071	0.0014

The average grain size is about 50μm, with a great scatter on the distribution of size per grain. The tensile stress-strain data as well as the creep constitutive laws are given in the **Table 2.**

2.2. Test procedures

Six creep crack initiation tests were carried out on normalized CT25 specimens which present two different geometries at the crack-tip : machined notch with a tip radius less than 100μm (CT n°22,23,33,39) and fatigue precrack at room temperature (CT n°52,53).

These creep tests (**Table 3**) were performed at 650°C on a servo-mechanical "MAYES" machine. Load point displacements $\delta(t)$ were measured by using extensometer attached to the specimens. Crack lengths a(t) were measured by the DC potential drop technique. The initiation time Ti was determined from a(t) data, as the time necessary for the crack to grow from the initial crack front over a critical distance d = 50μm, and tests were stopped after only about 150μm crack growth. CT specimens were then fatigue opened, and fracture surface were examined with scanning electron microscope.

3.NUMERICAL AND ANALYTICAL CALCULATIONS

3.1.Numerical calculations

CASTEM 2000 finite element code [4] was used to perform numerical simulations of the loading (elastic-plastic calculations), and the creep tests, until $t \approx Ti$. The calculation conditions are as follows :

- Plane strain, with Von Mises criterion ;
- Small deformation and large geometry changes ;
- very fine meshes (5μm size) at the neighbourhood of the crack tip **(fig.1)**.

3.2.Singularities at the crack tip

In the literature, the stress distribution at the crack tip is controlled by some loading parameters which deal with the state of the specimen during the test. Rice [5] showed that J is the loading parameter in elastic-plastic conditions. Riedel [6] found, for creeping conditions, C^*_h and C^* loading parameters, according to respectively extensive primary and secondary creep. The stress distribution in the vicinity of the crack tip can be expressed as :

$$\sigma_{ij} = \left(\frac{C_k}{B_k I_{n_k} r} \right)^{\frac{1}{n_k+1}} \tilde{\sigma}(\theta, n_k), \text{ where } I_{n_k} = 10.3 \sqrt{0.13 + \frac{1}{n_k}} - \frac{4.8}{n_k} \qquad [7] ;$$

k = 0, 1 or 2 for respectively plasticity, primary or secondary creep ; C_k is the adequate loading parameter ; r is the distance from the crack-tip ; B_k and n_k are given in **Table 2** (n_0 = n) ; $\tilde{\sigma}$ is a tabulated angular term [2].

J, C^*_h and C^* loading parameters are defined by using contour integrals but several "simplified methods" were proposed to evaluate them. In this text, we use especially the simplified method proposed by the "Ecole des Mines de PARIS" (referred to as EMP simplified method[8]) which is based on reference length (L_{ref}). This method deals with the assumption that the behaviour of a cracked specimen is similar to an uniaxial tensile bar of length L_{ref}, submitted to an applied reference stress σ_{ref}. The characteristic length L_{ref} was fitted in such a way that the calculated load point displacement were in good agreement with the measured value. L_{ref} was then found to be proportional to the remaining ligament : $L_{ref} = \gamma (W - a)$.

4.RESULTS

4.1. Experimental results

Experimental initial conditions of tests performed on CT specimens are given in **Table 3**, where we have also included the initial values of reference stress (σ_{ref}) calculated from limit-load analysis by MILLER [9], under Von Mises plane strain conditions :

$$\sigma_{ref} = \frac{F}{BWm\left(\frac{a}{W}\right)} ; \quad m\left(\frac{a}{W}\right) = 1.155 \left[-\left(1 + 1.702 \frac{a}{W}\right) + \sqrt{2.702 + 4.599 \left(\frac{a}{W}\right)^2} \right]$$

In this text, all numerical and theoretical calculations were made from CT53 specimen. F = 12kN and Ti = 110hours.

4.2. Comparison of global parameters

For the initial loading (elastic-plastic conditions), one can show the evolution of the applied load F versus δ (load-line displacement). In **fig.2** comparison is made between experimental points and both finite element and analytical calculations. Because the specimens have the same initial crack length, experimental points are the average points from all of six creep tests. Notice that the same experimental F versus δ curve was obtained for "machined" and "precracked" CT specimens.

Compared to experimental points, finite element code underestimates the load-line displacement under plane strain hypothesis and overestimates it, in plane stress condition. We assumed plane strain condition because of the thickness of CT specimens (B = 25mm). However, this hypothesis leads to lower values of δ, and parameters which depend directly on it.

According to reference length concept [9], $\delta = \gamma\,(W\text{-}a)B_0\sigma_{ref}^{n}$; where $\gamma = 13.6$ for Von Mises plane strain conditions, was adjusted from primary creep data. One can see in the **fig.2** the curve calculated with this method. There is no elastic part in the curve due to the non linear elastic behaviour assumed.

As J is proportional to δ, similar comparison results should be expected by using finite element and simplified methods.

During the actual creep test, constant load is maintained. Then, we can compare the evolution of load-line displacement creep component $\delta_c(t)$ (**fig.3**). The EMP simplified formula [9] is : $\delta_c(t)=\gamma(W\text{-}a)B_1\sigma_{ref}^{n1}t^{p1}$, ($\gamma$ = 13.6). γ adjustement was done with this formula by using all creep tests. For CT53 test, this simplified simulation underestimates the experimental result δ_c^{exp}.

Finite element model underestimates severely $\delta_c(t)$, compared to δ_c^{exp}. We already noticed that it is due to the supposed plane strain conditions.

For CT n°53 (F=12kN see **Table 3**), calculations of global loading parameters J_{exp}, J(EMP), J(FE), C^*_h and C^* are summarized as follows :

- J(FE) was obtained by CASTEM2000 finite element code [4] ; J(FE)=4.14N.mm^{-1}.

- $J_{exp} = 2\dfrac{n}{n+1}\dfrac{F}{B(W-a)}\delta_{exp}$ [ref.8] ; Jexp = 7.51N.mm^{-1}.

- $C_k(EMP) = 2\gamma\dfrac{n_k}{n_k+1}\dfrac{F}{B}B_k\sigma_{ref}^{n_k}$ [ref 8] ; where the index k = 0, 1 or 2 for plasticity, primary or secondary creep ; C_k is the adequate loading parameter (J, C^*_h or C^*) and F is the load. For CT n°53, J(EMP)=10.54N.mm^{-1} ; C^*_h=0.5N.mm^{-1}.h^{-p1} and C^*=0.014N.mm^{-1}.h^{-1}.

4.3. Local stresses

Non Linear Elastic Fracture Mechanics (NLEFM) give the HRR stress field that can be compared with elastic-plastic finite element calculations. As results we show in **fig.4**, the largest principal stress σ_{yy} singularity, from the crack tip ($r = 0$) to $r = 10mm$ ($\theta = 0$)

σ_{yy} calculated with finite element code has its maximum value at $r \approx 10\mu m$. We can explain this as the blunting effect [10]. In fact, calculations were made with "large geometry changes formulation" so the code took into account blunting. In the same way, the code can include the bending effect in the ligament, thus when $r > 3mm$, σ_{yy} decreases and becomes negative (compression) at about 12mm from the crack tip. HRR field is available only in the logarithmic linear part of σ_{yy}-curve : ($10\mu m < r < 1mm$). On the one hand ($r < 10\mu m$), the HRR field does not take into account the blunting effect, on the other hand ($r > 1mm$) the HRR field represents only the stress singularity and neglects the non singular stress value.

The validity of HRR field ($10\mu m < r < 1mm$) is clearly shown when one compares σ_{yy} calculated by finite element method and the HRR stress field calculated with J(FE) (dashed line). Solid line is the HRR stress field calculated with J_{exp}. As J_{exp} calculation is related to experimental value (it does not suppose plane strain or plane stress conditions) this HRR field is probably the good singularity ahead of the crack tip.

HRR stress field calculated with J(EMP) overestimates the values of σ_{yy}. Nevertheless, the "scatter" on σ_{yy} is reduced very much compared with those of J

$$\text{Since : } \sigma_{ij} = \left(\frac{J}{B_0 I_n r}\right)^{\frac{1}{n+1}} \tilde{\sigma}(\theta, n), \quad \text{then : } \frac{\Delta\sigma_{ij}}{\sigma_{ij}} \approx \frac{1}{n+1}\frac{\Delta J}{J}$$

The variations with distance (**fig.5**) and time (**fig.6**) from the crack tip of the "numerical" stress fields obtained by finite element analysis have been compared to the "theoretical" ones deduced from the application of Fracture Mechanics of creeping solids.

Fig.5 shows the stress singularities at $t = Ti$ ($Ti = 110hours$ for CT n°53). Here "theoretical" and "numerical" stress fields are compared. RR field is available for $10\mu m < r < 1mm$. Finite element calculations underestimates σ_{yy} values due to the plane strain conditions (see also **fig.3** for load-line creep component comparison). At $r = 50\mu m$, the RR field calculated σ_{yy} is about 13% greater than finite element ones. Thus, both results are in good agreement and indeed, C^*_h is a good loading parameter for primary creep.

In **fig.6**, we compare the σ_{yy} stress at $50\mu m$ versus time. The finite element relaxation rate is lower than RR field ones. It depends on the stress initial value which is underestimated. σ_{yy} comparison during the large scale primary creep leads to a difference of about 13% (already given at $Ti = 110h$). This remark is relative to the same crack tip geometry (precracked specimen).

5.DISCUSSION

Global approach of the Fracture Mechanics for creeping solids correlates Ti with the loading parameter such as C^*_h or C^*. For 316L(N) stainless steel, many works have been done in this way [11][12]. Usually, $Ti.C^{*\alpha}$ is found to be a constant of the material.

In this paper, we are interested in a local approach based on correlation between Ti and σ_{yy}. Such approach is similar to nominal stress (σ_{nom}) versus time to failure (t_R), for smooth specimens. In this approach, σ_{yy} must be calculated at a characteristic distance d from the crack tip [1]. $d=50\mu m$ for obvious microctructural meanings : it is the average grain size, which can be related to creep crack initiation mechanisms [11].

In **fig.7**, we plot σ_{yy} at $d=50\mu m$, calculated by both finite element method, which take into account the crack tip radius for "machined specimens", and by RR field (available only for precracked specimens), versus initiation time. The four lowest points are corresponding to "machined specimens". We can compare the plots with the nominal stress (σ_{nom}) versus time to failure (t_R) curve for smooth specimen : the same trend is observed. The master curve (σ_{nom}-t_R) is conservative compared to Ti-σ_{yy} correlation. In fact, actual master curve should be higher than the plotted nominal stresses versus time to failure curve :

- -time to failure (t_R) for smooth specimens is controlled by ductile rupture mechanisms, whereas in cracked specimens, time to initiation (Ti) depends on intergranular mechanisms ; t_R is then underestimated compared with Ti ;
- -in **fig.7**, nominal stress which is correlated with time to failure, is the initial stress where there is neither correction with the deformation increase during the test, nor correction with the creep damage evolution.

On the other hand, instead of using σ_{yy}-stress, one can define a damage function which deals with parameters such as largest principal or equivalent stress or strain. For instance PIQUES [11] proposes an incremental creep damage law as : $dD = A\sigma_{yy}^{\alpha}\varepsilon_{eq}^{\beta}d\varepsilon_{eq}$ where A, α and β are material constants. As a matter of fact, for the present approach $\alpha = 1$ and $\beta = -1$.

6.CONCLUSION

1/ Six creep tests were carried out on normalized CT25 specimens. The comparison between the calculated largest principal stress σ_{yy} at the crack tip, shows that HRR and RR fields are in good agreement with finite element calculations when $10\mu m < r < 1mm$, and so, loading parameters such as J, C^*_h and C^* controll the stress singularities ahead of the crack tip.

2/ (t_R-σ_{nom}) correlation (where t_R is the time to failure for smooth specimens) is very conservative compared with (Ti-σ_{yy}) ones on creep crack initiation regimes. In fact, crack mechanisms and stress corrections considerations should bring (t_R-σ_{nom}) master curve nearer to (Ti-σ_{yy}) points.

REFERENCES

[1] Langer, B.F. in Pressure Vessel Engineering Technology (Ed R.W. Nichols) Applied Science Pub. Ltd, London 1971.

[2] Rice, J.R., Rosengren, G.F, Hutchinson, J.W., Journal of the Mechanics and Physics of Solids, Vol.16, 1968 pp.1-31.

[3] Riedel, H. and Rice, J.R., in Fracture Mechanics : Twelfth Conference, ASTM STP 700, Philadelphia, 1980, pp. 112-130.

[4] Millard, A. et al., Transactions of the 9th SMiRT, Vol.B, 1987 pp.127-130.

[5] Rice, J.R., Journal of Applied Mechanics, Vol.35, 1968, pp. 379-386.

[6] Riedel, H., Journal of the Mechanics and Physics of Solids, Vol.29, 1981 pp.35-49.

[7] Mc Clintock, F.A., in Fundamental Aspects of Structural Alloy Design, Eds. Jaffee, R.I. and Wilcox, B.A. Plenum, New York, 1977.

[8] Bensussan, P., Piques, R. and Pineau, A., in Nonlinear Fracture Mechanics : Vol.1-Time-Dependent Fracture, ASTM STP 995, Philadelphia, 1989, pp.27-54.

[9] Miller, A.G., International Journal of Pressure Vessel and Piping, Vol.32, 1988, pp. 197-327.

[10] Rice, J.R and Johnson, M.A., in Inelastic Behavior of Solids, M.F. Kanninen, W.E Adler, A.R Rosenfield, and R.I. Jaffee, Eds, McGraw-Hill Book Co., New York , 1970 pp. 641-672.

[11] Piques, R., in "Mechanics and mechanisms to crack initiation and growth under viscoplastic conditions in an austenitic stainless steel" Thesis Ecole Nationale Supérieure des Mines de Paris, 1989.

[12] Webster, G.A. and Austin, T.S.P., Fatigue Fract. Engng. Mater. Struct., Vol.15, No.11, 1992, pp. 1081-1090.

TABLE 2 -316L(N) Tensile stress-strain data and creep constitutive laws (650°C).

Young Modulus	0.2% Yield stress	Ultimate tensile stress
140600MPa	125MPa	360MPa

Plasticity		Primary creep			Secondary creep	
$\varepsilon = B_0 \sigma^n$	σ (MPa)	$\varepsilon = B_1 \sigma^{n1} t^{p1}$		σ (MPa)	$\dot{\varepsilon} = B_2 \sigma^{n2}$ (h^{-1})	σ (MPa)
B_0	n	B_1	n_1	p_1	B_2	n_2
$7.65.10^{-11}$	3.60	$6.78.10^{-11}$	5.47	0.48	$1.70.10^{-20}$	6.99

TABLE 3 - Creep test conditions (650°C) [p : precracked , m : machined]

Specimen number	a/W	Load (kN)	σ_{ref} (MPa)	Initiation time (hours)	Test duration (hours)
CT22	0.55m	15	119.3	24	66
CT23	0.55m	13.5	107.4	49	145
CT33	0.55m	12	95.5	222	697
CT39	0.55m	14.5	115.3	127	262
CT52	0.55p	14.5	115.3	54	258
CT53	0.55p	12	95.5	110	291

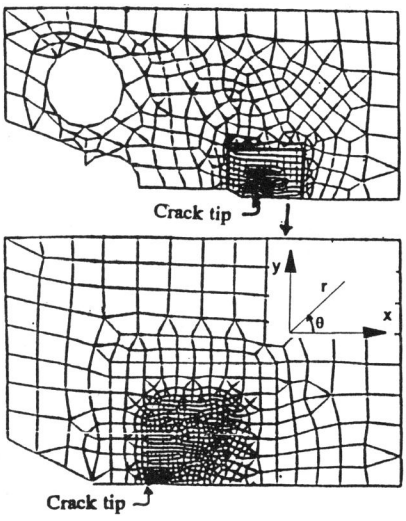

Fig.1:Finite element geometry

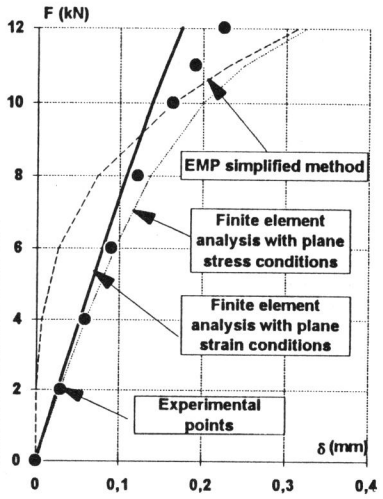

Figure 2:Elastic-plastic F vs δ curves

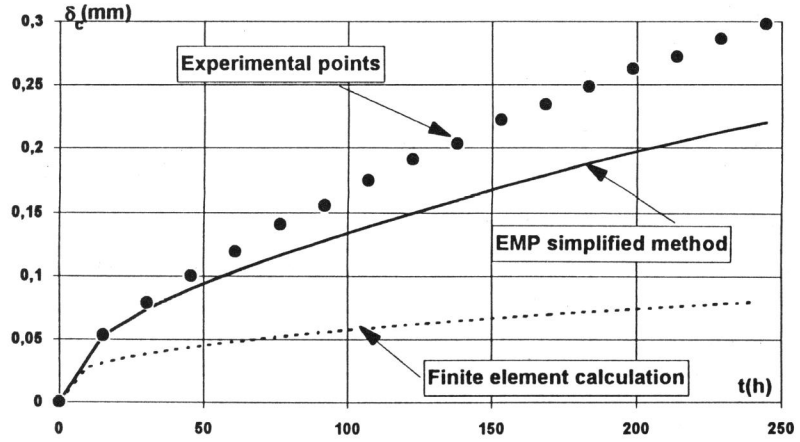

Figure 3 : Comparison of viscoplastic $\delta_c(t)$ curves

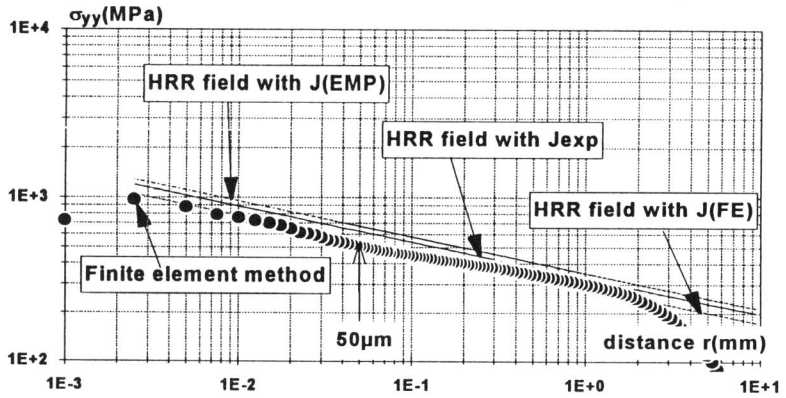

Figure 4: Theoretical and numerical largest principal stress distributions ahead of the crack tip. Lines are HRR stress fields with :
- J(EMP) : EMP simplified method with reference length
- J_{exp} : calculated with experimental (F, δ) curve
- J(FE) : calculated by finite element code CASTEM 2000

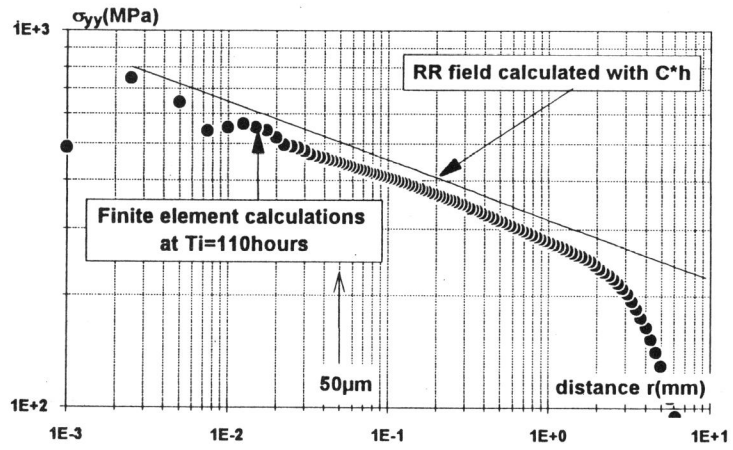

Figure 5: Theoretical and numerical largest principal stress distribution ahead of the crack tip

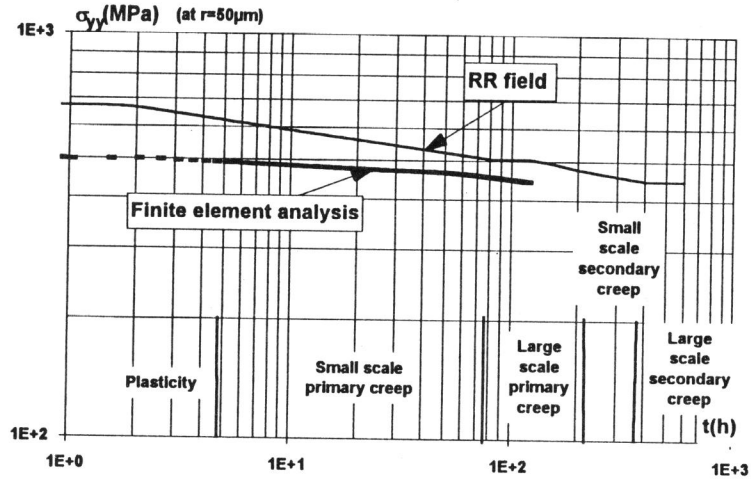

Figure 6: Theoretical and numerical relaxation of the largest principal stress σ_{yy}

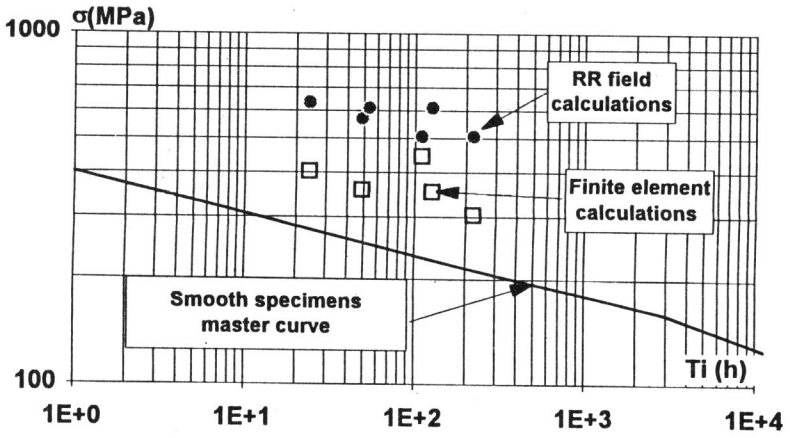

Figure 7 : Comparison between (σ_{nom} - t_R) and (Ti-σ_{yy}) correlations